Water Supply

Water Supply Vol 23 No 4, 1531 doi: 10.2166/ws.2023.069

Spatial and temporal trends of polyhalogenated carbazoles in sediments of the Yangtze river: insights into the origin

Chunnian Da[a,b,c,*], Peng Ji[a], Qinghui Huang[b], Jin Yu[a], Linjun Wu[a] and Jinsong Ye[a]

[a] School of Biology, Food and Environment, Hefei University, Hefei, Anhui Province 230022, China
[b] Key Laboratory of Yangtze River Water Environment, Ministry of Education, Shanghai 201804, China
[c] Anhui Key Laboratory of Sewage Purification and Eco-restoration Materials, Hefei 230088, China
*Corresponding author. E-mail: dachunnian2005@163.com

ABSTRACT

Fifteen surface sediments and three sediment cores were sampled in the Yangtze River (YR) of China to study the composition and temporal distribution trends of 10 selected polyhalogenated carbazoles (PHCZs) and gained insight into their origin. The total concentrations of PHCZs in the surface sediments ranged from 1.58 to 5.45 ng g^{-1} dry weight (dw), with an average of 3.11 ng g^{-1} dw. The composition profiles of PHCZs in the surface sediments were dominated by 1,3,6,8-tetrabromocarbazole, 1,3,6-dibromocarbazole, and 3,6-dichlorocarbazole. The variation trends of PHCZs in the sediment cores showed an apparent peak concentration and subsequently a significant decreasing trend in recent years. A strong correlation existed between PHCZs and sediment physicochemical properties. Furthermore, human activities directly or indirectly affected PHCZ concentrations. The evaluation of the potential toxic effect suggested that the toxic equivalent of PHCZs was less than the safe sediment value.

Key words: polyhalogenated carbazoles, temporal trends, toxic equivalent evaluation, Yangtze River

HIGHLIGHTS

- Polyhalogenated carbazoles (PHCZs) were detected in surface and core sediments from the Yangtze River.
- The composition profiles of PHCZs were dominated by 1,3,6,8-tetrabromocarbazole.
- PHCZs in the cores showed an apparent peak concentration and a significant decreasing trend in recent years.
- A strong correlation exists between PHCZs and sediment physicochemical properties.
- Human activities affected PHCZs concentrations.

GRAPHICAL ABSTRACT

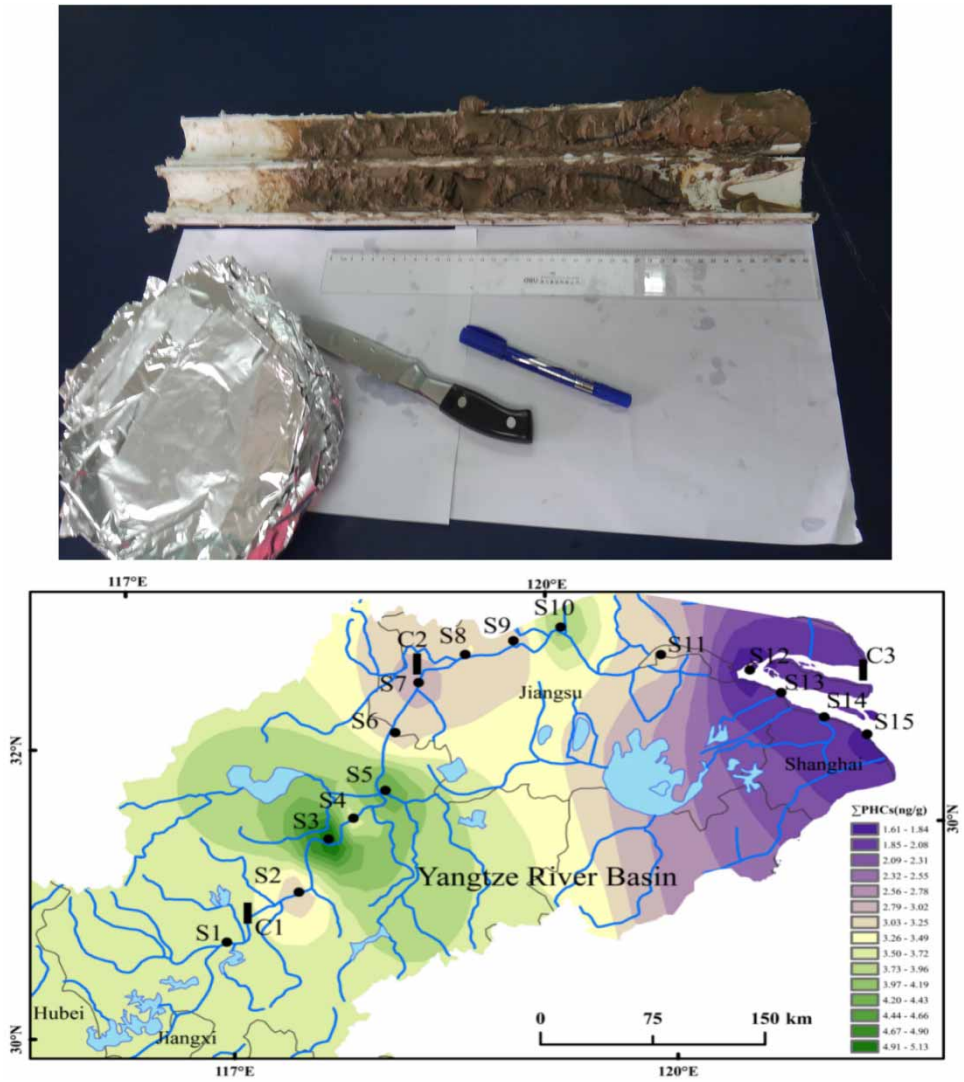

1. INTRODUCTION

Polyhalogenated carbazoles (PHCZs) have attracted increasing attention due to their mobility, toxicity, and semi-volatile nature that have raised environmental concerns globally (Riddell *et al.* 2015). Several recent studies (Wu *et al.* 2017b; Ji *et al.* 2019; Yue *et al.* 2020) have revealed that PHCZs exert bioaccumulation, biomagnification, and dioxin-like effects. As early as in the 1980s, the PHCZ 1,3,6,8-tetrachlorocarbazole was first discovered by Kuehl *et al.* (1984) in sediments from the Buffalo River of the USA, which suggested the existence of PHCZs in the aquatic environment. In recent decades, various studies have indicated the presence of PHCZs in sediments, soil, and air in different areas worldwide (Kronimus *et al.* 2004; Altarawneh & Dlugogorski 2015; Wu *et al.* 2016; Zhou *et al.* 2021). For example, 1,3,6,8-tetrabromocarbazole (1368-BCZ) and other halogenated carbazoles (including $ClBr_3$, $ClBr_4$, $ClBr_3I$, Br_4I, and Br_3I2-carbazole) have been detected in aquatic sediments from the Lippe River of Germany (Zhu *et al.* 2019), the North Sea Estuary of Germany (Zhou *et al.* 2021), Lake Michigan (Guo *et al.* 2014), the Saginaw River of the USA (Zhou *et al.* 2021), Ontario of Canada (Kronimus *et al.* 2004; Guo *et al.* 2014), Lake Tai of China (Eljarrat *et al.* 2005), the northern South China Sea (Zhou *et al.* 2021), and the Jiulong River of China (Zhou *et al.* 2019). The potential sources of these PHCZ congeners are not thoroughly documented (Pena-Abaurrea *et al.* 2014). Halogenated indigo dyes, optoelectronic materials, and p-chloroaniline structure herbicides have been suggested as the anthropogenic sources of some PHCZs. For example, 1368-BCZ may form as an

impurity in the manufacturing process of indigo dyes (Mumbo *et al.* 2015). In addition, some PHCZs may be produced from natural sources; for example, the marine fungus *Caldariomyces fumago* can synthesize BCZ in water with the help of enzymes (Kronimus *et al.* 2004; Xu *et al.* 2017). The discharge of saline wastewater containing PHCZs (e.g., brine) degrades water quality and thus water cannot be directly used for potable water (via desalination) and industrial applications (Ji *et al.* 2019). However, studies on the sources of PHCZs and the effect of the input volume of human activities on PHCZs have been limited yet. For instance, PHCZs were detected in unpolluted soil from Germany and the sediment cores formed before 1900. Chen *et al.* (2018) suggested that PHCZs are widespread in the depositional environment. The sediments have long been considered reservoirs of various organic pollutants. Although more and more studies have been conducted on the environmental sources of PHCZs, knowledge of their historical contamination in the aquatic environment and evaluation of toxic equivalency to organisms remains inadequate (Guo *et al.* 2017; Ji *et al.* 2019). Therefore, PHCZs' traceability and migration behavior in environmental media must be further investigated. Better understanding of aquatic systems is necessary to determine the occurrence and distribution characteristics of PHCZs as well as their correlations with anthropogenic factors in a region.

The Yangtze River (YR) with a length of 6,387 km runs across central China from west to east. It flows through eight provincial regions in China and into the east China Sea to the east of Chongming Island. Most cities on both sides of the YR are China's industrial centers and crucial economic driving forces. Therefore, the YR is polluted by the industrial development of coastal cities (Da *et al.* 2020). Because of human activities, it is one of the most affected rivers in the world. The present study targets the section of the YR extending from the Anhui Province to Chongming Island; the districts in this section represent regions with the highest degree of industrialization and urbanization in China (Sun *et al.* 2016). To our knowledge, the presence of PHCZs in sediments of the YR has not been reported yet. This study aims to (1) study both the residual level and composition profiles of PHCZs in sediments of the YR, (2) analyze the historical variation tendency of PHCZs and anthropogenic factors in the sediment cores, and (3) determine the toxic effects of PHCZs in sediments.

2. MATERIALS AND METHODS

2.1. Sediment sampling

Three sediment cores were sampled with a gravity corer of 80-mm diameter in July 2018. The sampling sites are displayed in Figure 1. The geographic locations of the sites are as follows: 30°44′4.01″ (N) and 117°25′15.38″ (E) for core 1 (C1; length = 44 cm); 32°08′9.99″ (N) and 118°45′34.02″ (E) for core 2 (C2; length = 41 cm); and 31°37′0.3″ (N) and 121°50′26.74″ (E) for core 3 (C3; length = 40 cm). C1 is near the rural area in the Anhui Province; C2 is near Nanjing in the Jiangsu Province; and C3 is near the Yellow Sea. The sediment cores were cut into 1-cm segments from top to bottom. Every segment was wrapped and sealed in aluminum foils baked at a high temperature. Fifteen surface sediments (S1–S15) were sampled from 15 sites in July 2020. The surface sediment sampling process is described in detail in our previous study (Da *et al.* 2020). Briefly, the surface sediments (0–10 cm) were sampled with an iron grab. All surface sediment samples were labeled and kept at −20 °C in the laboratory before analysis.

2.2. Chemicals and reagents

Based on the previous studies (Wu *et al.* 2017a; Zhou *et al.* 2021), in this study, we selected 10 common PHCZs in the environment and purchased their standard mixtures from Cambridge Isotope Laboratories, Inc., USA. The selected PHCZs are as follows: 3-monochlorocarbazole (3-CCZ); 1,3,6,8-tetrabromocarbazole (1368-BCZ); 3,6-dichlorocarbazole (36-CCZ); 3,6-dibromocarbazole (36-BCZ); 2,3,6,7-tetrachlorocarbazole (2367-CCZ); 1,3,6-tribromocarbazole (136-BCZ); 1-bromo-3,6-dichlorocarbazole (1-B-36-CCZ); 1,3,6,8-tetrachlorocarbazole (1368-CCZ); 1,8-dibromo-3,6-dichlorocarbazole (18-B-36-CCZ); and 3-monobromocarbazole (3-BCZ). The chemical structures of the investigated PHCZ congeners are shown in Supplementary Figure S1. The toxicological information on PHCZs is listed in Supplementary Table S1. The surrogate standards (F-BDE69, F-BDE160, and PCB-204) and internal standards (F-BDE154 and DCDE) were purchased from Wellington Laboratories (Guelph, ON, Canada). Silica gel (100–200 mesh), sodium sulfate (Na_2SO_4), and neutral alumina (Al_2O_3) were purchased from Sigma-Aldrich (St. Louis, MO, USA), and they were baked at 400 °C for 16 h and stored at 200 °C before use.

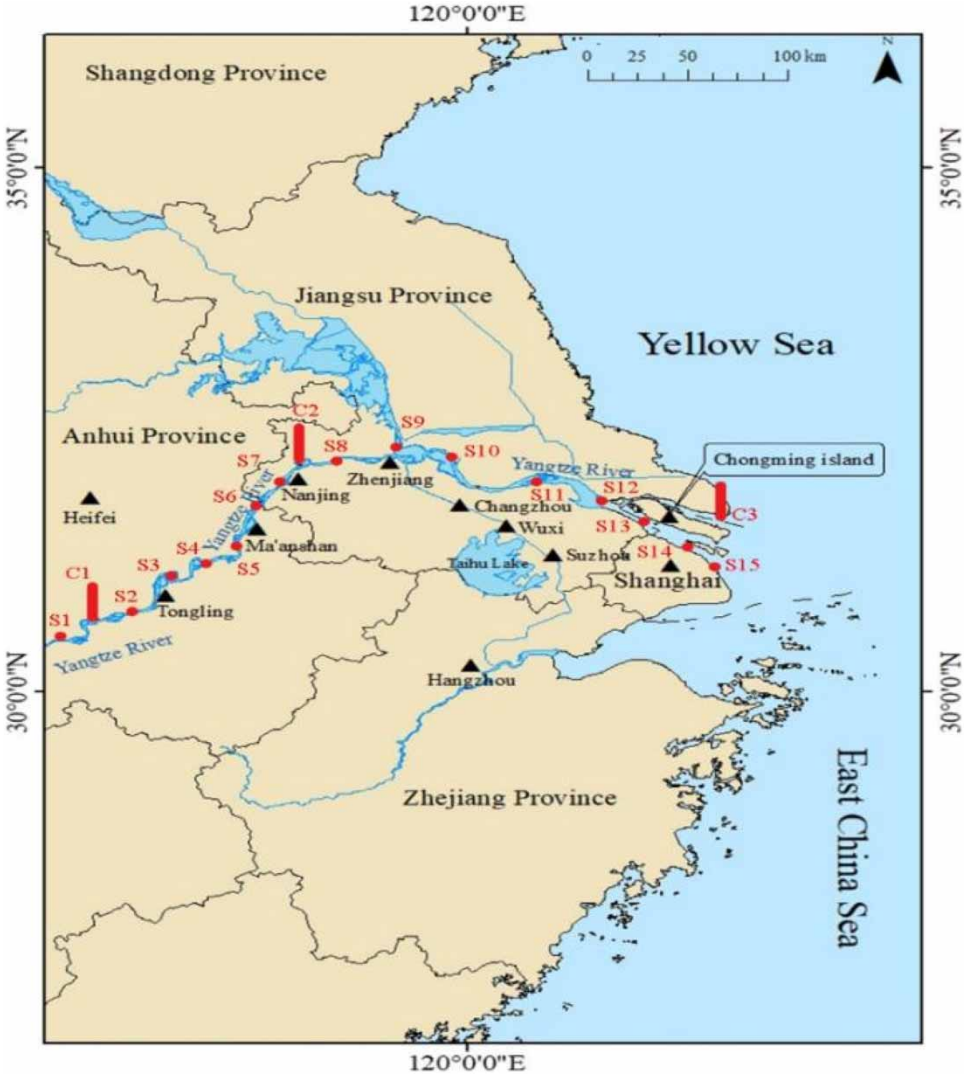

Figure 1 | Locations of sampling points.

2.3. Dating of sedimentary cores

The sediment dating procedure has been elaborated in a previous study (Da *et al.* 2020). Briefly, the core samples were freeze-dried at −200 °C, mixed evenly, and stored in vessels for 21 days to achieve equilibration of ^{226}Ra and its daughter isotope ^{210}Pb. ^{210}Pb, ^{137}Cs, and ^{226}Ra were quantified through γ-spectrometry at 46.1, 659, and 349 keV, respectively, by using Canbettra ultra-low-background germanium detectors. The dates were calculated using a constant supply rate date model (CRS) (Da *et al.* 2021):

$$t(i) = \frac{1}{\lambda}\ln\left[\frac{A(0)}{A(i)}\right] \quad (1)$$

where t(i) denotes the date for the sediment formation at depth i; λ stands for the decay constant of ^{210}Pb; $A(0)$ is the total inventory of the ^{210}Pbex; and A(i) stands for the accumulated deposit of ^{210}Pb below depth i. Dates in the sediment cores calculated using the CRS model are shown in Supplementary Figure S2.

The counting statistical errors were higher than ±2.9%. The layers corresponded to years 1959–2017 spanning 58 ± 3.42 years in C1, 1962–2018 spanning 56 ± 3.40 years in C2, and 1959–2017 spanning 58 ± 3.39 years in C3. The average deposition rates for C1, C2, and C3 were 0.75, 0.80, and 0.78 cm y^{-1}, respectively.

2.4. Analysis of PHCZs

Referring to a previous study (Wu *et al.* 2016), analytical methods were used in the present study. The sediment samples were dehydrated through freeze drying at −200 °C for approximately 40 h in a freeze dryer (Jinteng, Tianjin, China), pulverized to <200 mesh, and then homogenized. To 8 g each of the homogenized sediment samples, 40 ng of the surrogate standard (F-BDE69) was added, and accelerated solvent extraction (Thermo Fisher Scientific, Inc.) was conducted with hexane and acetone mixture (1:1, v/v). A moderate amount of activated copper powder was used to remove sulfur in the concentrated sediment extract. After sulfur removal, the extract was characterized through high-performance liquid chromatography with a gel permeation chromatography column (250 mm × 18.9 mm, 4 um). The extraction solution was heated to 120 °C in four cycles, with heating for 10 min and then allowing the solution to stand for 10 min. The extracts were concentrated with a rotary evaporator and then dried and solvent-exchanged into l mL of hexane. A burette with a scale was filled from the top to the bottom with anhydrous Na_2SO_4 (length = 1.0 cm), alumina (length = 8.0 cm), silica gel (length = 4.0 cm), and anhydrous Na_2SO_4 (length = 4.0 cm). The hexane extract was added to the burette (baked at 240 °C before use) and eluted with 50 mL of hexane. It was then washed with a 100 mL mixture of hexane and dichloromethane (v/v = 4:1) and 100 mL of dichloromethane. The eluent was concentrated and placed in a 200 μL brown glass bottle for the subsequent analysis.

PHCZ concentrations were determined using an Agilent 1290 gas chromatography system coupled with an Agilent 5973 MS in the electron impact ionization mode. The target substances were analyzed on an HP-5MS column (100 mm i.d., 2.1 mm) and an injector protected in the pulsed-splitless mode at 250 °C. The starting temperature of the oven was kept at 30 °C for 5 min, which was increased to 100 °C at 5 °C min^{-1}, and then increased to 200 °C at 10 °C min^{-1} and maintained for 12 min. Three PHCZs, namely 3-CCZ, 3-BCZ, and 36-CCZ, were measured in the splitless mode, whether the other PHCZs were detected in the negative ion mode. Supplementary Figure S3 shows a chromatogram of the target PHCZs by using the selected SIM ions. The qualitative and quantitative ionic characteristics of each target compound are presented in Supplementary Table S2. According to the description in previous studies (Wu *et al.* 2016; Zhou *et al.* 2019), the PHCZs were identified and quantified based on the sample peaks, retention times, peak areas, and signal-to-noise ratios.

2.5. Determination of physicochemical parameters

The total organic carbon (TOC) concentration in the sediments was determined through combustion oxidation. For this analysis, 0.1 g of the sediment samples was weighed and placed in a beaker, to which phosphoric acid solution was added until all bubbles in the beaker disappeared. The samples were then placed in an EL Cube elemental analyzer (Elementar Analysensysteme GmbH, Langenselbold, Germany) to measure the values.

The particle sizes of the sediments were measured by sieving on meshes of different sizes and then categorized as follows: >0.3 mm, 0.1–0.3 mm, and <0.1 mm. The percentages of finer particles (particles size <0.1 mm) were calculated.

2.6. Quality control and quality assurance

To avoid the interference of pollutants, all glassware were pre-cleaned with ultrapure water and hexane, followed by roasting at 180 °C for 10 h before use. A procedural blank sample was analyzed after every five samples. No studied compounds were found in the blank samples. The surrogate recovery rates were 91.1 ± 2.3%, 89.5 ± 2.1%, and 94.3 ± 5.2% for F-BDE69, F-BDE160, and PCB-204, respectively. The mixed standards with individual PHCZs (10 ng g^{-1}) were injected into the samples without analytes. The limits of detection (LOD) were set as a signal-to-noise ratio of 2. The relative standard deviation (RSD), LOD, and recoveries (R) of individual PHCZ congeners are shown in Supplementary Table S3.

2.7. Data analysis

SPSS AMOS 21.0 was used for the statistical analysis. The principal component analysis (PCA) was performed with Kaiser normalization and a factor adjustment of 2. *T*-test was performed to determine significant differences in the level of PHCZs among different samples.

3. RESULTS AND DISCUSSION

3.1. PHCZs in the surface sediments

3.1.1. Occurrences of PHCZs

Table 1 shows 10 target PHCZ congeners in the surface sediments from the YR. The detection rates of individual PHCZs ranged from 60 to 100% in the surface sediments, reflecting the ubiquitous occurrence of PHCZs in different regions of

Table 1 | Concentrations (ng g^{-1} dry weight) of PHCs in surface sediments

Sampling sites	3-CCZ	3-BCZ	36-CCZ	36-BCZ	1-B-36-CCZ	2367-CCZ	136-BCZ	1368-CCZ	18-B-36-CCZ	1368-BCZ	∑PHCs
S1	0.12	0.35	0.19	0.31	0.29	0.12	0.76	0.66	0.11	0.65	3.56
S2	0.19	0.13	0.43	0.21	0.11	0.33	0.45	0.33	0.13	0.67	2.98
S3	0.30	0.23	0.56	0.99	0.34	0.43	0.78	0.65	0.19	0.98	5.45
S4	0.23	0.21	0.16	1.01	0.66	0.34	0.43	0.27	ND	0.12	3.43
S5	0.29	0.10	1.10	0.65	0.12	0.11	0.22	0.66	0.08	1.21	4.54
S6	0.17	ND	0.91	0.54	0.33	0.28	0.19	0.15	0.12	0.33	3.02
S7	0.16	ND	0.31	0.39	0.12	0.43	0.55	0.43	0.09	0.31	2.79
S8	0.23	0.11	0.31	0.41	0.56	0.21	0.33	0.11	0.34	0.66	3.27
S9	0.16	0.08	0.45	0.38	0.11	0.41	0.54	0.09	ND	0.78	3.00
S10	0.34	ND	0.12	0.29	0.09	0.65	0.56	0.12	0.56	1.32	4.05
S11	0.31	ND	0.13	ND	0.07	0.54	0.45	0.33	0.34	0.98	3.15
S12	0.22	0.09	0.45	0.11	ND	ND	0.12	0.03	ND	0.56	1.58
S13	0.09	0.08	0.66	0.09	0.04	0.05	0.33	0.09	0.22	0.33	1.98
S14	0.11	ND	0.54	ND	ND	0.01	0.57	0.17	0.12	0.55	2.07
S15	0.07	ND	0.47	0.08	ND	0.04	0.78	0.11	ND	0.12	1.71
Detection rate (%)	100	60	100	86.67	80	93.33	100	100	73.33	100	–
Mean	0.20	0.09	0.45	0.36	0.19	0.26	0.47	0.28	0.15	0.64	3.11

the YR. All 10 target PHCZ congeners were detected in all samples. The detection rates for 3-CCZ, 36-CCZ, 136-BCZ, 1368-CCZ, and 1368-BCZ in all the samples were up to 100%, whereas that for 2367-CCZ was up to 93.33%, indicating that these compounds were the predominant contaminants in the surface sediments. The detection rate for 3-BCZ was much less than those for the other compounds, possibly because 3-BCZ was not stable and tended to be further halogenated into other PHCZ congeners (Zhou *et al.* 2021). Moreover, the total concentration of PHCZs ranged from 1.58 to 5.45 ng g^{-1}, with a mean value of 3.11 ng g^{-1}. The comparison of PHCZ distribution in various regions of the world (Supplementary Table S4) indicates that the mean concentrations (i.e., 3.11 ng g^{-1}) of PHCZs in the YR were higher than those in the surface sediments sampled from the northern South China Sea and Lake Tai of China but lower than those in the surface sediments sampled from the Jiaozhou Bay wetland of China, Jiulong Estuary of China, Saginaw River system of the USA, North Sea Estuary of Germany, Great Lakes of the USA, and San Francisco Bay of the USA. The occurrences of compounds in various regions suggest wide distributions of the compounds in global aquatic ecosystems.

Compared with other persistent organic pollutants in the YR, the mean levels of PHCZs were lower than those of polybrominated diphenyl ethers (PBDEs; 378 ng g^{-1}) (Da *et al.* 2020), organochlorine pesticides (OCPs; 45.8 ng g^{-1}) (Gong *et al.* 2020), and polycyclic aromatic hydrocarbons (PAHs; 4,002 ng g^{-1}) (Li *et al.* 2020) but higher than that of polychlorinated biphenyls (PCBs; 1.98 ng g^{-1}) (Guo *et al.* 2021).

3.1.2. Composition characteristics of PHCZs

The composition characteristics of PHCZ congeners are shown in Figure 2. Among the 10 detected individual PHCZ congeners in the surface sediments from the YR, 1368-BCZ dominated the composition profile, followed by 136-BCZ and 36-CCZ, accounting for 50.47% of ∑PHCZ in the surface sediments. However, other individual congeners accounted for more than 10% of the total. The dominance of 1368-BCZ in the YR conforms to the composition characteristics of PHCZs detected in the northern South China Sea (Ji *et al.* 2019). Previous studies have shown that rich bromide ions could result in the dominance of 1368-BCZ in the aquatic environment. The lower-brominated carbazoles tend to transform the higher-brominated congeners into rich bromide ions of the aquatic environment (Altarawneh & Dlugogorski 2015). According to Zhu *et al.* (2019), approximately 500,000 aquatic animals and bacteria can promote the natural biosynthesis of organichalogen compounds in the aquatic environment. Therefore, distinguishing the sediments containing high bromine ions in the YR is difficult. Leri *et al.* (2014) reported that bromination is ubiquitous in the environment, stimulating the conversion of low-brominated carbazoles to high-brominated homologs.

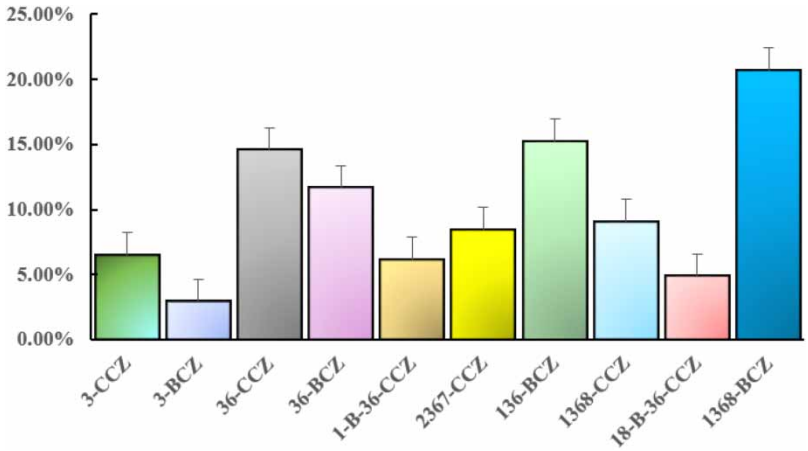

Figure 2 | The composition profiles of polyhalogenated carbazoles in surface sediments.

In addition, Kuehl *et al.* (1984) discovered an elevated concentration of 1368-BCZ near the outfall of a former dye manufacturer. 136-BCZ was reported to be an intermediate product of photoelectric materials (Parette *et al.* 2015). Therefore, this study deduced that brominated carbazoles emerged from anthropogenic sources in the study area. This composition profile differs from that obtained from the investigation of sediments in Lake Tai, where 36-CCZ and 36-BCZ were the major congeners, while 1368-BCZ had relatively less contribution. Of the PHCZs in Lake Tai sediments, the contribution of 36-CCZ and 36-BCZ was 97.31%, whereas 3-BCZ and 1368-BCZ accounted for up to 1.91 and 1.92%, respectively. In addition, 36-CCZ was found to be predominant in the Saginaw Bay River and the coastal North Sea (Zhou *et al.* 2021). The dominance of 36-CCZ in various aquatic systems may be related to the electrophilic aromatic substitution mode, which is conducive to halogen substitution on carbazole relative to the *ortho* and *para* positions of nitrogen (Zhou *et al.* 2021).

3.1.3. Spatial distribution patterns of PHCZs

The spatial distribution patterns of PHCZs are shown in Figure 3. An apparent concentration variation trend of PHCZs can be observed from downstream to upstream in the YR. Elevated concentrations of PHCZs were found in the midstream (Anhui section) of the YR. Peak concentrations of PHCZs were detected in the sediments sampled from S3 (averaged at 5.45 ng g^{-1}), followed by S5 (averaged at 4.54 ng g^{-1}). Field investigation revealed that there was a printing and dye factory in the past near

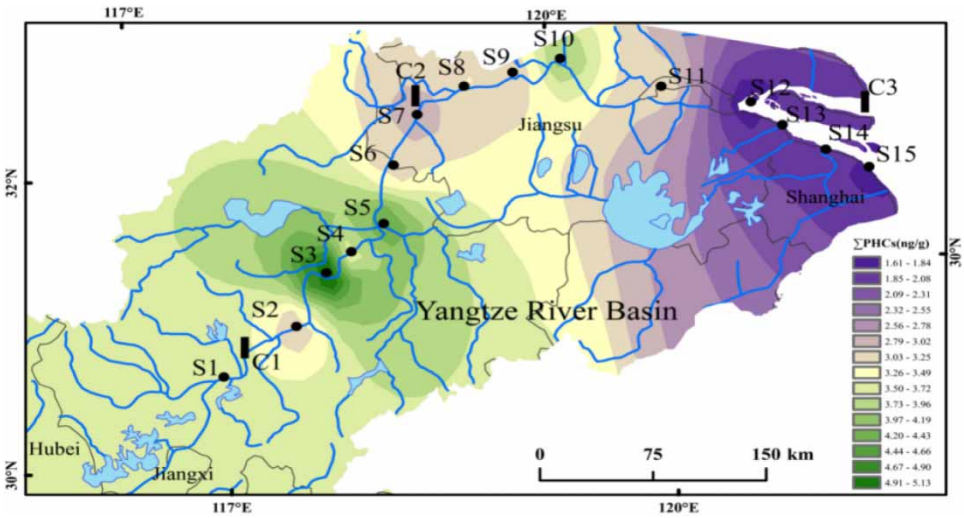

Figure 3 | Spatial distributions of PHCs in sediments.

S3 in Maanshan City, which contributed to high residual levels in the nearby river basin. Parette *et al.* (2015) reported that 1368-BCZ might be a by-product in the production of halogenated indigo dyes. Kuehl *et al.* (1984) strongly supported that high residual levels of 1368-CCZ were found in the discharge around the dye factory. Furthermore, the results of this study verified the pollution pathway of the anthropogenic sources of PHCZs. The lowest concentrations of PHCZs were observed in S12 (averaged at 1.58 ng g^{-1}), followed by S15 (averaged at 1.71 ng g^{-1}). The concentrations of PHCZs differ by a factor of 3.44, indicating an apparent degree of variation according to the environmental gradient. Notably, a decreasing trend of PHCZ content was observed in the downstream of the YR. S12 and S15 are near the Yellow Sea; thus, PHCZs are easily washed away with seawater. In addition, some other factors (e.g., physicochemical properties of sediments) may account for the difference in PHCZ concentrations across different sampling sites.

3.2. PHCZs in the sediment cores

3.2.1. Occurrences of PHCZs

To study the sedimentary characteristics of PHCZs, the variation trend of vertical concentrations of PHCZs during different years was analyzed in the three sediment cores from the YR. As shown in Table 2, the detection rates of individual PHCZs were 43.18–95.45% in C1, 46.34–88.80% in C2, and 42.50–90.00% in C3. The three sediment cores displayed high detection rates, which indicated the widespread use of PHCZs historically. Overall, all 10 target PHCZ congeners were detected in all the samples. 36-CCZ, 36-BCZ, and 1368-BCZ dominated the composition profile in the three cores and were also observed in the surface sediments collected from the YR. Moreover, the residual levels of ∑PHCZs were 0.01–3.07 ng g^{-1} (average: 1.06 ng g^{-1}) for C1, 0.01–2.91 ng g^{-1} (average: 0.83 ng g^{-1}) for C2, and 0.01–2.61 ng g^{-1} (average: 0.84 ng g^{-1}) for C3. The mean and detection rates of the individual PHCZs in C1 were higher than those in C2 and C3. The difference in the residual levels of ∑PHCZs in the three cores was mainly attributed to the different geographic locations and surrounding human activities, which also account for their high concentration in surface sediments of site S3; the dye factory was approximately 10 km from C1, leading to the residual levels of ∑PHCZs in C1.

3.2.2. Temporal profiles of PHCZs

Figure 4 shows the temporal profiles of the residual levels of PHCZs in the cores. In the core profiles, the recorded PHCZ residues undulated with the sedimentary ages. The variation trends of PHCZs in sediment cores have shown an apparent peak concentration and subsequently a significant decreasing trend in recent years. The total concentrations of PHCZ congeners were found at low residues in the deep sediment layers before the 1980s. This variation trend of PHCZs is similar to that of PBDEs in the cores from the YR reported in our previous studies (Da *et al.* 2020). The variation trend of PHCZs in C3 differed slightly from those of C1 and C2. The residual levels of PHCZs across C1 and C2 increased continuously until 1990–2008 and decreased toward the surface layers of the sediment. The concentration of PHCZs in C1 and C2 peaked

Table 2 | Concentrations (ng g^{-1} dry weight) of PHCs in sediment cores

	Core S1 (Depth:44 cm)			Core S2 (Depth:41 cm)			Core S3 (Depth: 40 cm)		
Compounds	**Range**	**Mean**	**Detection rate (%)**	**Range**	**Mean**	**Detection rate (%)**	**Range**	**Mean**	**Detection rate (%)**
3-CCZ	0.01–0.66	0.27	68.18	0.04–0.31	0.13	56.10	0.01–0.32	0.09	42.50
3-BCZ	0.09–1.01	0.59	63.63	0.02–0.78	0.45	80.00	0.01–1.56	0.39	62.50
36-CCZ	0.19–2.18	1.56	90.91	0.08–2.07	1.39	85.36	0.21–1.89	1.36	85.00
36-BCZ	0.34–3.18	2.01	95.45	0.21–2.88	1.56	82.92	0.14–2.61	1.87	75.00
1-B-36-CCZ	0.06–1.09	0.78	50.00	0.32–1.45	0.39	53.65	0.02–1.29	0.38	42.50
2367-CCZ	0.05–1.13	0.43	43.18	0.16–1.41	0.51	70.73	0.15–1.01	0.54	67.50
136-BCZ	0.01–1.78	0.99	54.55	0.04–1.99	1.01	46.34	0.21–1.23	0.67	72.50
1368-CCZ	0.06–1.89	1.01	72.72	0.01–1.07	0.63	70.73	0.01–1.31	1.04	47.50
18-B-36-CCZ	0.09–1.19	0.51	75.00	0.02–0.44	0.21	60.97	0.01–1.11	0.61	45.00
1368-BCZ	0.34–3.07	2.45	95.45	0.21–2.91	1.99	88.80	0.11–2.01	1.42	90.00
∑PHCs	0.01–3.07	1.06	70.45	0.01–2.91	0.83	69.56	0.01–2.61	0.84	63.00

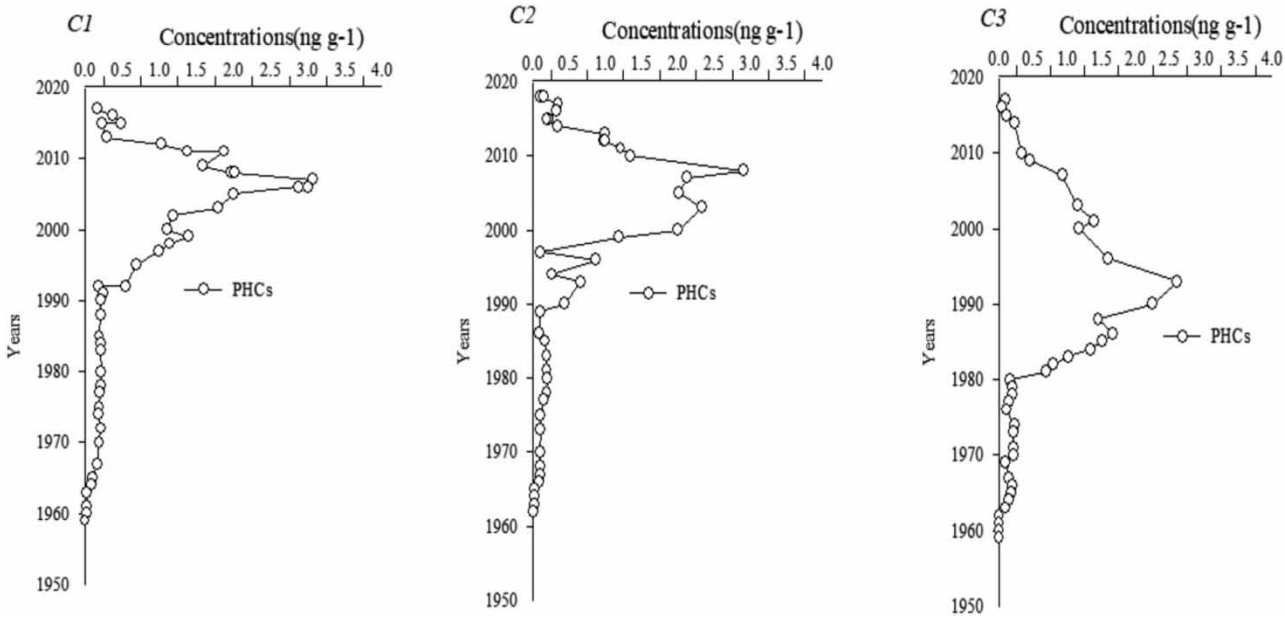

Figure 4 | Temporal trends of PHCs in the sediment cores.

in 2007 and 2008, respectively. However, the significant increase in the PHCZ concentration in C3 occurred 10 years earlier than that in C1 and C2, and in C3, there was an apparent increasing trend from 1980 to 1993. The concentrations of PHCZs peaked in C3 in 1993. C1, C2, and C3 were near the Yellow River in the Anhui Province, Jiangsu Province, and the Yellow Sea, respectively. C3 located at the Yellow River Sea Estuary is impacted frequently by the seawater turbulence with the influx of saline water, causing the bioaccumulation of cyanobacteria on PHCZs in the ocean. Lee *et al.* (1999) reported that cyanobacteria have a strong bioaccumulation ability and can absorb and accumulate PHCZs (Chen *et al.* 2016). In addition, our visit to the surrounding residents revealed that many dye plants existed near C3 in the 1990s. Therefore, possibly, PHCZs from those dye plants discharged into the YR through runoff during the 1990s, resulting in the deposition of PHCZs in C3. PHCZs in the three sediment cores displayed apparent peak residues and subsequently decreased significantly. The tortuous variation of PHCZs in the YR was similar to those reported in the cores sampled from Lake Michigan (Guo *et al.* 2014) but different from the stable variation trends of PHCZs found in the northern South China Sea (Zhou *et al.* 2021).

3.2.3. Composition characteristics of PHCZs

Supplementary Figure S4 indicates that slightly different from the congener composition profiles found in the surface sediments, the predominant PHCZs of the three cores in various sedimentary times were 36-CCZ, 36-BCZ, and 1368-BCZ, accounting for more than 50% of the total PHCZs. The ratios of the three compounds were 57–100%, 55–100%, and 31–100% in C1, C2, and C3, respectively. PHCZ concentrations in these three cores were less than those found in Lake Michigan and the Upper Great Lakes but greater than those found in the northern South China Sea (Guo *et al.* 2017; Zhou *et al.* 2021). Parette *et al.* (2015) reported that 1368-BCZ possibly originated from tetrabromodiiodine produced by the halogenated indigo dye factory. Additionally, in this study, 1368-BCZ was predominant among the 10 analyzed PHCZs in the three cores, suggesting that anthropogenic sources of PHCZs affected the historical compositions in the cores. The environmental source of 36-CCZ and 36-BCZ is not completely known (Zhu *et al.* 2019). According to some studies, they were formed from monuron or monolinuron, an intermediate product of optoelectronic materials and polymers that is biodegradable in nature (Mai *et al.* 2005; Mumbo *et al.* 2013). For example, PHCZs were believed to have originated from the natural biodegradation in the sediments from Lake Michigan and the northern South China Sea. Therefore, the relatively high concentrations of 36-CCZ and 36-BCZ suggest that the PHCZs in the study area originated likely from a natural source.

3.3. Factors influencing PHCZ patterns

To determine the factors affecting the distribution profiles of PHCZs in the YR, the relationship between TOC and the percentages of finer particles (particles size < 1 mm) and PHCZs was studied (Figure 5). A significant positive correlation was observed between PHCZs and sediment physicochemical properties (TOC and finer particles) because the finer particles have a large adsorption surface area for PHCZs. Although the pollution sources and complex hydraulic conditions in the YR at different locations are unknown, TOC showed positive correlations with PHCZs, indicating the possibility of

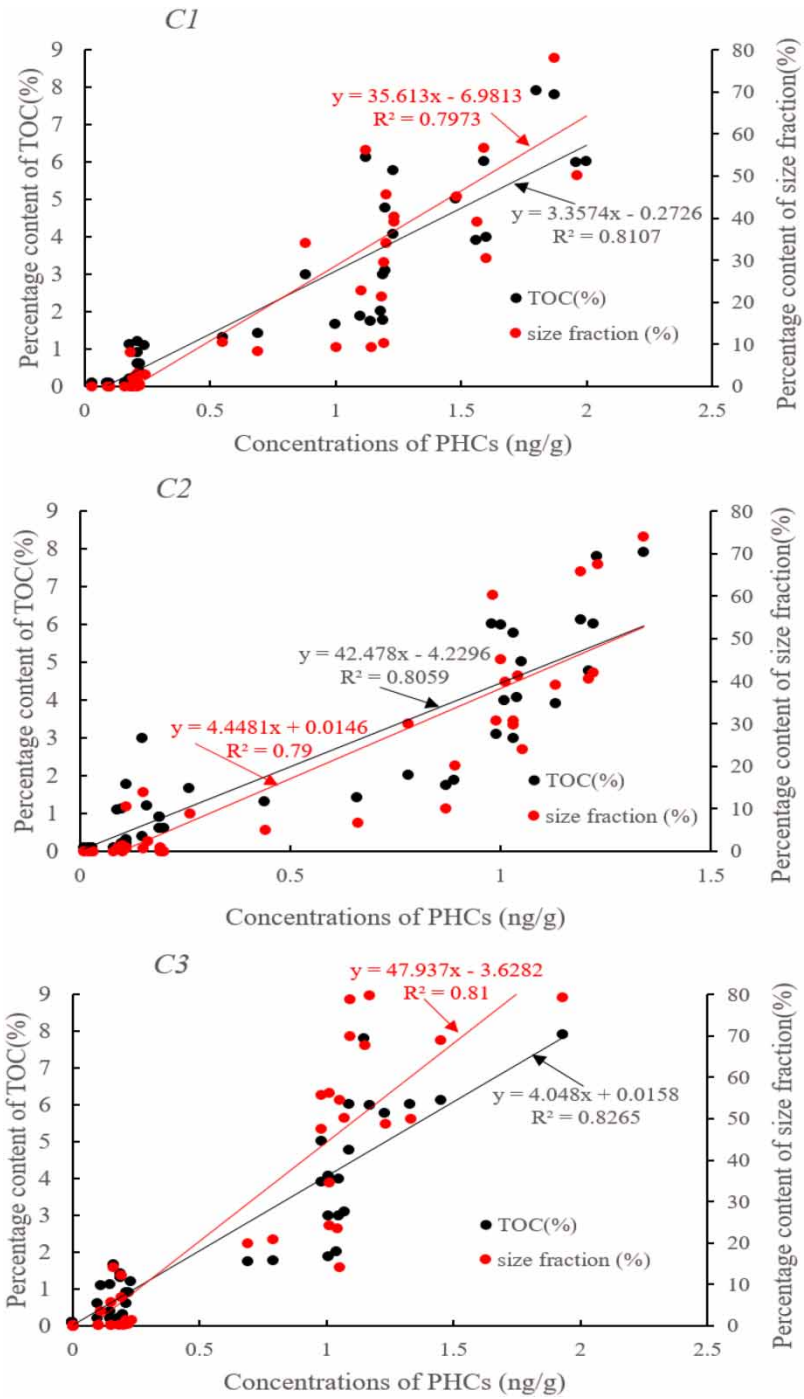

Figure 5 | Correlations between PHCs concentrations and percentage content of TOC and size fraction.

redistribution of PHCZs in the sediment cores. Previous studies on PAHs have also reported positive correlations between TOC, fine grain size, and PAH concentrations (Li *et al.* 2020). These results suggest that various factors affect the distribution of PHCZs in sediments from the YR. To further identify the factors that affect the source of PHCZs in the YR, a structural equation model (SEM) encompassing 15 anthropogenic factors and climatic factors (i.e., temperature) was used (the data were collected from http://www.stats.gov.cn). PCA was used to divide the 15 individual factors into six categories: urbanization, population, economic development, industrial structure, pollution emission, and transportation volume (Supplementary Table S5). The SEM results are displayed in Supplementary Figure S5. The hypothetical model agreed with our data: Chi-square (CS) = 0.01, comparative fit index (CFI) = 2.13, Tucker-Lewis index (TLI) = 14, goodness-of-fit index (GFI) = 0.98, Akaike information criterion (AIC) = 18, and root-mean-square error of approximation (RMSEA) = 0.02. Industrial structure ($\lambda = 0.37$, $P < 0.001$), population ($\lambda = 0.28$, $P < 0.01$), economic development ($\lambda = 0.29$, $P < 0.001$), and pollution emission ($\lambda = 0.19$, $P < 0.05$) positively affected PHCZs, whereas temperature, urbanization, and transportation volume had no direct effects on PHCZs. Although temperature had no direct effect on PHCZ concentrations, it had a positive effect on pollution emission, indicating that it indirectly affected PHCZ concentrations as pollution emission can positively affect PHCZ concentration. We have also reported that PBDEs in Huaihe River was closely related to economic development and population (Da *et al.* 2021). Therefore, it was not difficult to speculate that population, economic development and pollution emission were important sources affecting PHCs in the YR.

As shown in Supplementary Table S5, PCA was applied to show the rotated component matrix of anthropogenic parameters. The result indicated that 96.04% of the data variation could be explained by the first six components. The principal component factor of the total variance was distinguished by the high positive loadings of total population, urbanization, GDP, sewage, per capital GDP, the ratio of heavy industry, ratio of light industry, and industrial wastewater emission. The presence of these anthropogenic parameters suggests a strong correlation with PHCZs.

3.4. Toxic effects of PHCZs

The toxic effects of PHCZs are calculated according to the following formula (Wu *et al.* 2017b):

$$\mathrm{TEQ} = \sum (Ci * \mathrm{REP}i) \tag{2}$$

where TEQ is the toxic equivalent of the PHCZs, Ci is the residue levels of individual PHCZ congeners (ng g^{-1}, dry weight (dw)), and REPi is the relative effect potencies of individual PHCZ congeners, as determined by Riddell *et al.* (2015), which are presented in Supplementary Table S6.

As shown in Supplementary Table S6, the evaluated TEQ values of PHCZs in surface sediments from the YR ranged from 25.6×10^{-5} to 107.2×10^{-5} ng g^{-1} (mean = 60.57×10^{-5} ng g^{-1}), which was lower than the safe sediment value of 0.020 ng g^{-1} (Zhu *et al.* 2019). The comparatively high TEQ values of PHCZs were detected in the sediments at sites S3 and S5, where the high residue levels of 1368-CCZ were observed. Comparison with the other regions indicates that the TEQ values of PHCZs in sediments from the YR were higher than those from Lake Tai of China (0–140×10^{-5} ng g^{-1}, mean = 10×10^{-5} ng g^{-1}) (Wu *et al.* 2017a), Jiaozhou Bay wetland of China (10×10^{-5}–390×10^{-5} ng g^{-1}, mean = 110×10^{-5} ng g^{-1}) (Zhu *et al.* 2019), and San Francisco Bay of the USA (20×10^{-5}–180×10^{-5} ng g^{-1}, mean = 120×10^{-5} ng g^{-1}) (Wu *et al.* 2017b). Although the TEQ values of PHCZs in sediments from the YR were relatively low, synergistic, or superposition effects caused by the coexistence of PHCZs and other persistent toxic pollutants such as dioxin PCB, PBDEs, and PAHs cannot be ruled out (Yan *et al.* 2017). Therefore, the existence of PHCZs in sediments and their harmful effects on aquatic organisms necessitate further research in the field.

4. CONCLUSION

This study revealed the spatial and temporal trends of the distribution of PHCZs in the cores and surface sediments obtained from the YR, China. The analysis results indicated a ubiquitous distribution of PHCZs in the sediments from the YR, and their residue levels were comparable to those of the other prominent organic pollutants such as OCPs, PCBs, and PBDEs. The compositions and distribution profiles suggested that a combination of natural and anthropogenic sources contributed possibly to the sediments of the YR. PHCZs and sediment physicochemical properties (including TOC and finer particles) were found to have a strong correlation. Moreover, human activities were found to directly or indirectly affect PHCZ concentrations. The evaluation of the toxicity of PHCZs suggested that the toxic equivalent of PHCZs was less than that of the

safe sediment. The applicability of the findings will understand the pollution of YR aquatic systems. The harmful effects of PHCZs on aquatic organisms must be investigated in future research.

ACKNOWLEDGEMENTS

This work was supported by Anhui Provincial Natural Science Foundation (2008085MD119), Hefei Municipal Natural Science Foundation (2021011), the Project Supported by Anhui Postdoctoral Fund (2019b332), and the Key Project of Anhui University Scientific Research Project (KJ2019A0826).

DATA AVAILABILITY STATEMENT

All relevant data are included in the paper or its Supplementary Information.

CONFLICT OF INTEREST

The authors declare there is no conflict.

REFERENCES

Altarawneh, M. & Dlugogorski, B. Z. 2015 Formation and chlorination of carbazole, phenoxazine, and phenazine. *Environ. Sci. Technol.* **49**, 2215–2221. https://doi.org/10.1021/es505948c.

Chen, W., Xie, Z., Wolschke, H., Gandrass, J., Kotke, D., Winkelmann, M. & Ebinghaus, R. 2016 Quantitative determination of ultra-trace carbazoles in sediments in the coastal environment. *Chemosphere* **150**, 586–595. https://doi.org/10.1016/j.chemosphere.2016.02.051.

Chen, Y., Lin, K., Chen, D., Wang, K., Zhou, W., Wu, Y. & Huang, X. 2018 Formation of environmentally relevant polyhalogenated carbazoles from chloroperoxidase-catalyzed halogenation of carbazole. *Environ. Pollut.* **232**, 264–273. https://doi.org/10.1016/j.envpol.2017.09.045.

Da, C., Wang, R., Xia, L., Huang, Q., Cai, J., Cai, F. & Gao, C. 2020 Sediment records of polybrominated diphenyl ethers (PBDEs) in Yangtze River Delta of Yangtze River in China. *Mar. Pollut. Bull.* **160**, 111714. https://doi.org/10.1016/j.marpolbul.2020.111714.

Da, C., Wang, R., Huang, Q., Mao, J., Xie, L., Xue, C. & Zhang, L. 2021 Sediment records of polybrominated diphenyl ethers (PBDEs) from the Anhui Province section of Yangtze River, China. *Bull. Environ. Contam. Toxicol.* **106**, 334–341. https://doi.org/10.1007/s00128-020-03054-x.

Eljarrat, E., De La Cal, A., Larrazabal, D., Fabrellas, B., Fernandez-Alba, A. R., Borrull, F., Marce, R. M. & Barcelo, D. 2005 Occurrence of polybrominated diphenylethers, polychlorinated dibenzo-p-dioxins, dibenzofurans and biphenyls in coastal sediments from Spain. *Environ. Pollut.* **136**, 493–501. https://doi.org/10.1016/j.envpol.2004.12.005.

Gong, X., Li, Q., Zhang, L., Zhao, Z., Xue, B., Yao, S. & Cai, Y. 2020 The occurrence of organochlorine pesticides (OCPs) in riverine sediments of hilly region of southern China: implications for sources and transport processes. *J. Geochem. Explor.* **216**, 106580. https://doi.org/10.1016/j.gexplo.2020.106580.

Guo, J., Chen, D., Potter, D., Rockne, K. J., Sturchio, N. C., Giesy, J. P. & Li, A. 2014 Polyhalogenated carbazoles in sediments of Lake Michigan: a new discovery. *Environ. Sci. Technol.* **48**, 12807–12815. https://doi.org/10.1021/es503936u.

Guo, J., Li, Z., Corcoran, M. B., Hosseini, S. & Li, A. 2017 Spatial and temporal trends of polyhalogenated carbazoles in sediments of upper great lakes: insights into their origin. *Environ. Sci. Technol.* **51**, 89–97. https://doi.org/10.1021/acs.est.6b06128.

Guo, F., Yin, S., Wang, H., Zhang, J., Liu, Y., Aamir, M. & Liu, W. 2021 Polychlorinated biphenyls (PCBs) in the colostrum samples from the Yangtze River Region: exposure profile and risk assessment. *Environ. Pollut.* **285**, 117253. https://doi.org/10.1016/j.envpol.2021.117253.

Ji, C. Y., Shen, C., Zhou, Y. X., Zhu, K. Y., Sun, Z., Zuo, Z. H. & Zhao, M. R. 2019 Ahr agonist activity confirmation of polyhalogenated carbazoles (PHCZs) using an integration of in vitro, in vivo, and in silico models. *Environ. Sci. Technol.* **53**, 14716–14723. https://doi.org/10.1021/acs.est.9b05388.

Kronimus, A., Schwarzbauer, J., Dsikowitzky, L., Heim, S. & Littke, R. 2004 Anthropogenic organic contaminants in sediments of the Lippe River. *Ger. Water Res.* **38**, 3473–3484. http://dx.doi.org/10.1016/j.watres.2004.04.054.

Kuehl, D. W., Durhan, E., Butterworth, B. C. & Linn, D. 1984 Tetrachloro-9H-carbazole, a previously unrecognized contaminant in sediments of the Buffalo River. *Great. Lakes Res.* **10**, 210–214. https://doi.org/10.1016/S0380-1330(84)71827-2.

Lee, S. C., Williams, G. A. & Brown, G. D. 1999 Maculalactone L and three halogenated carbazole alkaloids from *Kyrtuthrix maculans*. *Phytochemistry* **52**, 537–540. https://doi.org/10.1016/S0031-9422(99)00226-5.

Leri, A. C., Mayer, L. M., Thornton, K. R. & Ravel, B. 2014 Bromination of marine particulate organic matter through oxidative mechanisms. *Geochim. Cosmochim. Acta* **142**, 53–63. https://doi.org/10.1016/j.gca.2014.08.012.

Li, B., Zhou, S., Wang, T., Zhou, Y., Ge, L. & Liao, H. 2020 Spatio-temporal distribution and influencing factors of atmospheric polycyclic aromatic hydrocarbons in the Yangtze River Delta. *J. Clean Prod.* **267**, 122049. http://dx.doi.org/10.1016/j.jclepro.2020.122049.

Mai, B., Chen, S., Chen, S., Luo, X., Chen, L., Yang, Q., Sheng, G., Peng, P., Fu, J. & Zeng, E. Y. 2005 Distribution of polybrominated diphenyl ethers in sediments of the Pearl River Delta and adjacent South China Sea. *Environ. Sci. Technol.* **39**, 3521–3527. https://doi.org/10.1021/es048083x.

Mumbo, J., Lenoir, D., Henkelmann, B. & Schramm, K. W. 2013 Enzymatic synthesis of bromo- and chlorocarbazoles and elucidation of their structures by molecular modeling. *Environ. Sci. Pollut. Res.* **20**, 8996–9005. https://doi.org/10.1007/s11356-013-1823-6.

Mumbo, J., Henkelmann, B., Abdelaziz, A., Pfister, G., Nguyen, N., Schroll, R., Munch, J. C. & Schramm, K. W. 2015 Persistence and dioxin-like toxicity of carbazole and chlorocarbazoles in soil. *Environ. Sci. Pollut. Res.* **22**, 1344–1356. https://doi.org/10.1007/s11356-014-3386-6.

Parette, R., McCrindle, R., McMahon, K. S., Pena-Abaurrea, M., Reiner, E., Chittim, B., Riddell, N., Voss, G., Dorman, F. L. & Pearson, W. N. 2015 Halogenated indigo dyes: a likely source of 1,3,6,8-tetrabromocarbazole and some other halogenated carbazoles in the environment. *Chemosphere* **127**, 18–26. https://doi.org/10.1016/j.chemosphere.2015.01.001.

Pena-Abaurrea, M., Jobst, K. J., Ruffolo, R., Shen, L., McCrindle, R., Helm, P. A. & Reiner, E. J. 2014 Identification of potential novel bioaccumulative and persistent chemicals in sediments from Ontario (Canada) using scripting approaches with GCxGC-TOF MS analysis. *Environ. Sci. Technol.* **48**, 9591–9599. https://doi.org/10.1021/es5018152.

Riddell, N., Jin, U. H., Safe, S., Cheng, Y., Chittim, B., Konstantinov, A. & McCrindle, R. 2015 Characterization and biological potency of mono-to tetra-halogenated carbazoles. *Environ. Sci. Technol.* **49**, 10658–10666. https://doi.org/10.1021/acs.est.5b02751.

Sun, J. T., Pan, L. L., Zhan, Y., Lu, H. N., Tsang, D. C. W., Liu, W. X., Wang, X. L., Li, X. D. & Zhu, L. Z. 2016 Contamination of phthalate esters, organochlorine pesticides and polybrominated diphenyl ethers in agricultural soils from the Yangtze River Delta of China. *Sci. Total Environ.* **544**, 670–676. http://dx.doi.org/10.1016/j.scitotenv.2015.12.012.

Wu, Y., Moore, J., Guo, J., Li, A., Grasman, K., Choy, S. & Chen, D. 2016 Multi-residue determination of polyhalogenated carbazoles in aquatic sediments. *J. Chromatogr A* **1434**, 111–118. https://doi.org/10.1016/j.chroma.2016.01.036.

Wu, Y., Qiu, Y., Tan, H. & Chen, D. 2017a Polyhalogenated carbazoles in sediments from Lake Tai (China): distribution, congener composition, and toxic equivalent evaluation. *Environ. Pollut.* **220**, 142–149. https://doi.org/10.1016/j.envpol.2016.09.032.

Wu, Y., Tan, H., Sutton, R. & Chen, D. 2017b From sediment to top predators: broad expo-sure of polyhalogenated carbazoles in San Francisco Bay (U.S.A.). *Environ. Sci. Technol.* **51**, 2038–2046. https://doi.org/10.1021/acs.est.6b05733.

Xu, X., Wang, D., Li, C., Feng, H. & Wang, Z. 2017 Characterization of the reactivity and chlorinated products of carbazole during aqueous chlorination. *Environ. Pollut.* **225**, 412–418. https://doi.org/10.1016/j.envpol.2017.03.002.

Yan, W., Tan, H., Sutton, R. & Da, C. 2017 From sediment to top predators: broad exposure of polyhalogenated carbazoles in San Francisco Bay (U.S.A.). *Environ. Sci. Technol.* **51**, 2038. https://doi.org/10.1021/acs.est.6b05733.

Yue, S., Zhang, T., Shen, Q., Song, Q. & Zhao, M. 2020 Assessment of endocrine-disrupting effects of emerging polyhalogenated carbazoles (PHCZs): in vitro, in silico, and in vivo evidence. *Environ. Int.* **140**, 105729. https://doi.org/10.1016/j.envint.2020.105729.

Zhou, W., Huang, X. & Lin, K. 2019 Analysis of polyhalogenated carbazoles in sediment using liquid chromatography–tandem mass spectrometry. *Ecotox. Environ. Safe* **170**, 148–155. https://doi.org/10.1016/j.ecoenv.2018.11.131.

Zhou, W., Chen, W., Li, P., Gu, Z., Peng, J. & Lin, K. 2021 Occurrence and distribution of polyhalogenated carbazoles (PHCZ) in sediments from the northern South China Sea. *Sci. Total Environ.* **753**, 142072. https://doi.org/10.1016/j.scitotenv.2020.142072.

Zhu, H., Zheng, M., Zheng, L., Wang, L., Lou, Y. & Zhao, Q. 2019 Distribution and ecotoxicological effects of polyhalogenated carbazoles in sediments from Jiaozhou Bay wetland. *Mar. Pollut. Bull.* **146**, 393–398. https://doi.org/10.1016/j.marpolbul.2019.06.078.

First received 19 May 2022; accepted in revised form 24 February 2023. Available online 7 March 2023